IEEE Access
Multidisciplinary | Rapid Review | Open Access Journal

Received August 31, 2021, accepted September 3, 2021, date of publication September 7, 2021,
date of current version September 17, 2021.

Digital Object Identifier 10.1109/ACCESS.2021.3111027

Optimal Allocation/Sizing of DGs/Capacitors in Reconfigured Radial Distribution System Using Quasi-Reflected Slime Mould Algorithm

SAUBHAGYA RANJAN BISWAL[1], (Member, IEEE), GAURI SHANKAR[1], (Member, IEEE), RAJVIKRAM MADURAI ELAVARASAN[2,3,4], AND LUCIAN MIHET-POPA[5], (Senior Member, IEEE)

[1]Department of Electrical Engineering, Indian Institute of Technology (ISM) Dhanbad, Dhanbad, Jharkhand 826004, India
[2]Department of Electrical and Electronics Engineering, Thiagarajar College of Engineering, Madurai 625015, India
[3]Clean and Resilient Energy Systems (CARES) Laboratory, Texas A&M University, Galveston, TX 77553, USA
[4]Research and Development Division (Power and Energy), Nestlives Pvt. Ltd., Chennai 600091, India
[5]Faculty of Engineering, Østfold University College, 1757 Halden, Norway

Corresponding authors: Gauri Shankar (gaurishankar@iitism.ac.in), Rajvikram Madurai Elavarasan (rajvikram787@gmail.com), and Lucian Mihet-Popa (lucian.mihet@hiof.no)

ABSTRACT Increased load demands worsen distribution system problems such as greater line losses, voltage deviation and a plethora of other concerns. This current work presents an approach stressing simultaneous optimal allocation and sizing of capacitor banks and distributed generations, as well as optimal radial distribution system (RDS) reconfiguration, to address these difficulties. The above objectives are accomplished through the maiden application of the proposed quasi-reflection-based slime mould algorithm (QRSMA). The efficacy of QRSMA is established by testing it on different benchmark functions. A new modified backward forward load flow approach is also proposed and validated by comparing its results to those obtained using MATPOWER software for IEEE 69, 85, and 118 bus RDSs. The proposed load flow technique is independent of the sequential bus numbering scheme and may be applied to any RDS network topology. The proposed QRSMA is tested on 118 bus RDS and to prove its effectiveness; its results are compared to those of other studied algorithms. The study takes into account both fixed and variable loading scenarios. A cost-benefit analysis of the strategy is also performed in order to make the methodology more realistic.

INDEX TERMS Capacitor banks, distributed generation, network reconfiguration, quasi-reflection-based slime mould algorithm, radial distribution system.

I. INTRODUCTION

An electrical distribution system serves as a link between generating units and consumers. With the growing load demand and expanding distribution system networks, line losses are increasing and bus voltages have become more vulnerable. As a result, it has become critical for the power utility sectors to solve such issues while taking into account numerous economic and environmental factors. Many researchers have examined options such as optimal placements of distributed generations (DGs) and capacitor banks (CBs) and distribution system reconfiguration in the past for power loss reduction, voltage profile improvement and distribution system reliability enhancement [1]. However, their improper placements may affect the system negatively *i.e.*, it may result in increased line losses and voltage instability. Therefore, the optimal DG and CB placements (ODGCBP) are given a significant weightage for the proper planning of the electrical distribution systems [2]. Generally, radial distribution systems (RDS) are widely used, consisting of normally closed sectionalize switches and normally open tie switches. When necessary, some of the sectionalize switches can be opened by closing the equal number of tie switches in order to divert the load feeding path without jeopardizing the distribution system's radial structure. The proper optimal reconfiguration of the radial distribution system (RDS) can reduce line losses

The associate editor coordinating the review of this manuscript and approving it for publication was Bilal Alatas.

while also improving voltage stability and load balancing [3]. As a result, the simultaneous ODGCBP and optimal reconfiguration (OR) of the RDS aid in alleviating the aforementioned problems.

The load flow analysis technique is generally utilized to obtain various network parameters such as bus voltage, line losses, branch currents, etc. In recent years, a number of load flow techniques have been proposed by researchers in search of accurate results and quick convergence for RDS. Among them, conventional methods like Newton-Raphson, Gauss-Seidel and fast-decoupled load flow methods fail to offer the efficient solution and fast convergence because of the high resistance to reactance ratio of radial distribution lines [4]. In [5], the authors have iteratively solved three equations for updating voltage and power flow at each bus of the RDS. Whereas, in [6], Goswami and Basu presented a method in which the network topology is converted into a defined format and then the system parameters are obtained. The claimed method is found to be only valid for the networks having one incoming and a maximum of two outgoing branches, making it an unrealistic approach. A backward forward sweep method is proposed in [7] to obtain the line losses and bus voltages of RDS. But, in this approach, the scheme of sequential numbering of buses is necessary for finding accurate results. A direct load flow approach is proposed in [8], which has attracted many researchers due to its simplicity and quick convergence. In this method also, the sequential numbering of nodes is must and, thus, makes it unsuitable for changing network topology. It may be inferred that when the network configuration changes, the above-mentioned methodologies are unable to give satisfactory results. Furthermore, several of the approaches described use matrix calculations, which impose a significant computational burden in large distribution networks. Hence, as a solution to the above problem, in this work, a new branch current update-based modified backward forward load flow approach is proposed, which is capable of offering an accurate and quick solution for any modified topology of RDS. In addition, the proposed approach does not require any matrix calculation, which fastens its computational time.

Recently, several analytical and artificial intelligence approaches have been adopted by many researchers to solve the ODGCBP problem along with OR of RDS. In [9], the authors have utilized grasshopper algorithm to obtain an optimal allocation of fixed and switchable CBs in RDS using power loss index and graph set theory. Authors in [10], proposed three different hybrid optimization algorithms for solving optimal placement of CBs and their switching schedule. An approach for the optimal allocation and sizing of multiple DGs based on optimally varying their power factor

TABLE 1. Summary of existing literatures in comparison with the proposed work.

Reference Number	Year of Publication	Techniques	Configuration	Objective Function	DG power factor; Loading condition
[9]	2019	Grass shopper algorithm	CB	B	-; Variable
[10]	2020	Genetic algorithm, Exchange market algorithm and Particle swarm optimization	CB	A	-; Variable
[11]	2020	Differential evolution-based algorithm	DG	B	Optimized; Variable
[12]	2020	Jaya algorithm	DG	B+C	Fixed; Fixed
[13]	2021	Analytical model	DG	B+C	Fixed; Variable
[14]	2020	Improved harris hawks optimizer	DG	B+C	Fixed; Fixed
[15]	2016	Genetic algorithm, Particle swarm optimization	DG	B+C+D	Optimized; Fixed
[16]	2020	Plant propagation algorithm	DG	B+C	Fixed; Fixed
[17]	2020	Analytical model	DG	A	Fixed; Variable
[18]	2019	Genetic algorithm	DG-CB	B+C	Fixed; Variable
[19]	2019	Analytical model	DG-CB	B	Optimized; Variable
[20]	2021	Analytical model	Reconfiguration	B	-; Variable
[21]	2021	Analytical model	Reconfiguration	B	-; Fixed
[22]	2019	Mixed integer programming	CB-Reconfiguration	A	-; Variable
[23]	2020	Improved sine cosine algorithm	DG-Reconfiguration	B+C	Fixed; Variable
[24]	2020	Three dimensional group search optimization approach	DG-Reconfiguration	B	Fixed; Variable
[25]	2020	Moth flame algorithm	DG-Reconfiguration	B+C+D	Optimized; Fixed
[26]	2021	Mixed integer linear programming	DG-Reconfiguration	C	Fixed; Variable
[3]	2017	Hybrid harmony search algorithm-particle artificial bee colony algorithm	DG-CB-Reconfiguration	B+C	Fixed; Variable
[27]	2017	Bacterial foraging optimization	DG-CB-Reconfiguration	B+C	Fixed; Fixed
[28]	2020	Thief and police algorithm	DG-CB-Reconfiguration	A+ B+C	Fixed; Fixed
[29]	2020	Modified binary gray wolf optimization	DG-CB-Reconfiguration	B	Fixed; Variable
Proposed method	-	Quasi-reflection slime mould algorithm	DG-CB-Reconfiguration	A+ B+C+D	Optimized; Variable

In the 5th column, the A, B, C, D parameters refer to the system cost, power losses, voltage deviation and reliability index, respectively; and in the 6th column an entry '-' means not applicable.

is presented in [11]. In [12], the researcher utilized the Jaya algorithm to find the optimal placement of DGs comprising photovoltaic (PV) panels. In the above works, cost-benefit analysis has been ignored. Comprehensive analytical expressions are used in [13] for the placement of DG having multiple PV units by maximizing the technical benefits. The objective function considered in this work is composed of active power losses, reactive power losses, bus voltage deviations, line congestion margin and voltage stability index. The work presented in [14] highlights the application of both single and multi-objective Harris hawks optimization method to solve the optimal DG placement problem and also examines the economic viability of the obtained solutions. However, in this approach, fixed/constant load demand is considered. The optimal DG allocation using genetic and particle swarm optimization algorithms is presented in [15]. The objective function formulated for the studied optimization methodology aims towards active and reactive power losses reduction, improvement in bus voltage profile and high reliability index of the system. The plant propagation algorithm is used in [16] for the optimal deployment of the DGs by simultaneously maximizing the total active power loss reduction and upgrading the magnitude of bus voltages. In [17], a two-stage game-theoretic approach is employed for residential PV panels placement planning integrated with the energy shaving mechanism to increase financial benefits. The researchers in [18] have shown that the simultaneous optimal allocation and sizing of DGs and CBs yields better results than the individual allocation of these devices under variable loading conditions. Apart from this, cost-benefit evaluation is also reported. But, in this study, the number and power factor of the DGs are pre-assumed before applying the optimization process. In [19], for reactive power loss minimization, optimal placement and sizing of multi-type DGs and CBs are determined using generic closed-form analytical expressions. However, the cost-benefit analysis of the proposed approach is overlooked in this study. A convex mixed-integer conic programming model is presented in [20] to solve OR problem for RDS to reduce the system losses and improve the bus voltage profiles of the system. In [21], a global optimum flow pattern-based search algorithm is proposed for finding OR of unbalanced RDS to minimize the total system loss. A cost-effective method employing mixed-integer second-order cone programming for simultaneous optimal CB placements and reconfiguration of RDS is presented in [22]. An improved sine cosine algorithm (SCA) is utilized to obtain the optimal placement and sizing of DGs along with OR in [23]. But, the cost-benefit analysis and the effect of load variation were ignored in the presented work. In [24], integer, continuous, and binary type variables are utilized, respectively, for DGs' location, DGs' operating point and open/close state of switches during the optimization process to determine the optimal DG placement and OR of RDS under variable loading conditions. This study also ignores the cost-benefit investigation. Moth flame algorithm is used in [25] to solve the optimal placement of DGs, consisting of solar and wind energy sources, and OR of RDS with an aim to achieve power loss reduction, voltage deviation minimization and system reliability enhancement. The optimal allocation of DGs is obtained in [26] using a mixed-integer linear programming method by maintaining minimal line losses. Moreover, the OR is also found to further boost system performance. In [3], Muthukumar and Jayalalitha have applied a hybrid approach comprising harmony search algorithm and particle artificial bee colony algorithm for ODGCBP along with OR in RDS without considering the economic viability of the approach. A combination of a fuzzy multi-objective approach and bacterial foraging optimization technique is employed in [27] to determine OR and allocation and sizing of DGs and CBs in RDS. The analysis on the economic feasibility aspect of the approach and the impact of variable loading scenarios are overlooked in this work. Tolabi *et al*. [28] have proposed a new thief and police algorithm and used it for solving ODGCBP and the OR issues considering fixed loading scenarios. The economic analysis is also carried out. In [29], an optimal interaction between adopted DG, Volt-VAr devices and RDS reconfiguration is examined for energy-saving purposes using a modified binary gray wolf optimization approach. As surfaced from the literature, it has been found that very few works have been done on simultaneous optimal allocation and sizing of DGs and CBs along with OR of RDS. This motivates the present authors to further explore the problem of simultaneous ODGCBP and OR of RDS under variable loading conditions. To highlight the contribution of the paper, the comparison of existing literature with the proposed approach is illustrated in Table 1.

It is observed that the majority of past studies have failed to include a cost-benefit analysis. The solutions reported in those works are technically efficient, but they may or may not be economical. In addition, in most studies, DG power factor is pre-assumed as a fixed value. Hence, in this work, instead of pre-assuming a fixed value of power factor and the number of DGs, these parameters are derived using the proposed optimization algorithm. This makes the approach more efficient and advantageous. Also, cost-benefit analysis of ODGCBP along with the OR (which is not previously reported) under variable loading conditions is thoroughly addressed in the present study. The formulated problem becomes complex combinatorial as it simultaneously optimizes the number, size, location of DGs (with variable power factor) and CBs along with OR of RDS. Therefore, an efficient optimization algorithm is needed to obtain the desired results. The literature survey reveals that metaheuristic optimization techniques are highly efficient in quickly getting the optimal solutions to various complex engineering/non-engineering problems [30]. In the present work, the studied issue is a complex combinatorial optimization problem and involves a high computational burden. Hence, it encourages the authors to utilize the power of the metaheuristic approach to solve the formulated problem. Moreover, in the past, many novel optimization algorithms have been modified and improved to their new versions having enhanced exploration and exploitation

capabilities, such as improved SCA [23], enhanced chaotic Jaya algorithm [31] and so on. Among various modifications suggested, the opposition-based learning approach is found to be relatively effective. However, as per [32], it is revealed that the concept of quasi-reflection-based learning approach gives even better performance than the opposition-based learning. The quasi-reflection-based learning approach is more efficient, requires less computational effort and offers a high probability of converging near to the optimum global solution. Recently introduced slime mould algorithm (SMA) has strong global search ability and yielded commendable results in solving various real-world problems in the past [33]. However, in some cases, this has exhibited early convergence. This motivates the present authors to propose a new improved version of SMA featuring quasi-reflection-based learning. The proposed novel quasi-reflection-based SMA (QRSMA) may effectively maintain a balance between exploitation and exploration phases of the optimization process so as to escape premature convergence. The effectiveness of QRSMA is tested using a variety of unimodal and multimodal benchmark test functions and the results are compared to those achieved by other existing powerful algorithms such as the whale optimization algorithm (WOA), the salp swarm algorithm (SSA) and the SCA. Thereafter, to further establish its superiority, the proposed QRSMA and other studied algorithms are used to solve the problem of optimal placement and sizing of DGs and CBs in RDS along with its OR. The results obtained confirm its superiority over other algorithms.

A. RESEARCH GAP

The following observations may be concluded based on the aforesaid literature survey:

- When the network configuration changes in a non-sequential way, very little attention has been made to load flow strategies that can yield good outcomes.
- Very limited works have been reported on finding simultaneous optimal allocation and sizing of DGs and CBs along with OR of RDS under variable loading conditions.
- It is also observed that most of the previous works ignore the cost-benefit analysis of their proposed methodology.
- In most of the studies, power factor of DGs to be allocated has been pre-assumed as a fixed value.
- To the best of the authors' knowledge, objective function comprising parameters such as power loss, voltage deviation, reliability index and the total system cost has been considered to solve ODGCBP and OR issues of RDS.
- QRSMA has never been used in solving ODGCBP and OR issues.

B. MAIN CONTRIBUTION

The main contributions of the present work are listed below.

- For the first time, an improved version of SMA *i.e.*, QRSMA is proposed and its performance is validated using different unimodal and multimodal benchmark test functions.
- An efficient modified load flow algorithm is proposed, which produces desirable results without depending on the network topology of RDS.
- Simultaneous optimal allocation and sizing of DGs and CBs and network reconfiguration considering various constraints is presented along with cost-benefit analysis of the proposed method.
- The number of DGs and CBs and the power factor of DGs are also optimized instead of pre-assuming them as fixed values.
- Variable loading along with the fixed loading scenarios are considered to make the approach more realistic.

The rest of this paper is organized as follows. In Section 2, the problem formulation and the various constraints considered in the proposed approach are presented. Section 3 focuses on the proposed modified load flow technique. The proposed QRSMA is described in Section 4. Results and discussion are presented in Section 5 followed by the conclusion in Section 6.

II. PROBLEM FORMULATION

This section covers the formulation of objective functions for the proposed work, as well as the various constraints to be considered.

A. OBJECTIVE FUNCTION

The main objective of the problem is to obtain the optimal deployment of DGs and CBs in conjunction with OR of RDS, considering a proper evaluation of both technical and economic aspects. The objective function formulated for the optimization method is given by (1)

$$OF = \frac{SC_a}{SC_b} \times w_1 + \frac{APLL_a}{APLL_b} \times w_2 + \frac{CVDa}{CVD_b} \times w_3 + \frac{RI_b}{RI_a} \times w_4 \quad (1)$$

where, SC_a and SC_b are the system costs, $APLL_a$ and $APLL_b$ are the active power line losses, CVD_a and CVD_b are the cumulative voltage deviations, RI_a and RI_b are the reliability indices of the system. The suffixes a and b signify the system parameters after and before (*i.e.*, base case) application of the proposed approach, respectively. w_1, w_2, w_3 and w_4 are the weightage factors and are taken as 0.5, 0.2, 0.2 and 0.1, respectively, for the studied method.

The system cost (SC_a) employing the proposed approach is calculated using (2)

$$SC_a = \sum_{t=1}^{ny} (Real(V_s.I_s^*).T - ENS_a).K_e.PWV^t - C_{ENS_a} + C_{cost} + DG_{cost} \quad (2)$$

where, ENS_a and C_{ENS_a} are the energy not supplied and its cost after applying the proposed approach, respectively. V_s is the slack bus voltage and I_s is the injected slack bus current, K_e is the average energy cost. PWV signifies the present worth value. The symbol '$*$' indicates the complex conjugate

value. The cost for energy not supplied (ENS) is expressed in (3)

$$C_{ENS} = K_i \times ENS \tag{3}$$

where, K_i is the cost per unit of energy not delivered. The total cost of the CBs includes the purchase, installation and operation costs and is taken from the work of [34] and is expressed by (4)

$$C_{cost} = K_{cp} \sum_{i=1}^{NCB} QC_i + K_{ci} \times NCB + K_{com} \times NCB \times PWV \tag{4}$$

where, $C_{\cos t}$ is the total cost of CBs. K_{cp}, K_{ci} and K_{com} represent the purchase, installation and operation and maintenance costs of CBs, respectively. NCB is the number of installed CBs. QC_i is the reactive power compensation offered by CB at bus i. The DG's installation, operation and maintenance costs are referred from the article [35] and are expressed in (5)

$$DG_{cost} = \sum_{i=1}^{NDG} K_{dgin} \,.\, DGC_i + \sum_{t=1}^{ny} \sum_{i=1}^{NDG} P_{DGi} \,.\, K_{dgom} \,.\, T \,.\, PWV^t \tag{5}$$

where, K_{dgin} are K_{dgom} are the installation and the operation and maintenance costs of DGs, respectively. DGC_i is the installation capacity of the ith DG. P_{DGi} is the active power produced by the ith DG. T is the number of hours in a year, ny is the project time period in years and NDG is the number of installed DGs. PWV obtained in terms of the inflation rate ($infr$) and interest rate ($intr$) is given by (6).

$$PWV = \frac{1 + infr}{1 + intr} \tag{6}$$

The system cost before applying the proposed approach (SC_b) is calculated using (7)

$$SC_b = \sum_{t=1}^{ny} (Real(V_s.I_s^*).T - ENS_b).K_e \,.\, PWV^t - C_{ENS_b} \tag{7}$$

where, ENS_b and C_{ENS_b} are the energy not supplied and its cost before applying the proposed approach, respectively.

The active and reactive power line losses (indicated by $APLL$ and $RPLL$, respectively) are obtained utilizing (8) and (9), in order

$$APLL = \sum_{i=1}^{TNB-1} I_i^2 R_i \tag{8}$$

$$RPLL = \sum_{i=1}^{TNB-1} I_i^2 X_i \tag{9}$$

where, I_i, R_i and X_i are the current, resistance and reactance of the ith branch, respectively.

The cumulative voltage deviation of the system is defined by (10)

$$CVD = \begin{cases} 0 & \text{if } 0.95 \le V_i \le 1.05 \\ \sum_{i=1}^{TNB} 1 - V_i & \text{else} \end{cases} \tag{10}$$

where, V_i is the ith bus voltage and TNB is the total number of system buses. The reliability index of the system is taken from the reference [15] and is defined by (11)-(12)

$$\text{Reliability Index } (RI) = 1 - \frac{ENS}{P_D} \tag{11}$$

$$ENS = L_F R_D \sum_{i=1}^{NB} \lambda_i \, |I_i| \, V_{rated} \tag{12}$$

where, P_D and ENS are the total power demand of the system and the energy not supplied, respectively. L_F is the load factor, R_D is the repair duration, λ_i is the failure rate of ith branch, I_i is the ith branch current and V_{rated} is the rated bus voltage of the system.

B. CONSTRAINTS

The objective function is optimized considering the following technical constraints.

1) EQUALITY CONSTRAINTS

The active and reactive power balance constraints are, respectively, given by (13) and (14)

$$\sum_{i=1}^{NDG} P_{DGi} + P_G - APLL = P_{LD} \tag{13}$$

$$\sum_{i=1}^{NDG} Q_{DGi} + \sum_{i=1}^{NCB} QC_i + Q_G - RPLL = Q_{LD} \tag{14}$$

where, P_G and Q_G are the active and the reactive power flows from the grid, respectively. P_{LD} and Q_{LD} are the total active and the reactive power load demands of the system, respectively. Q_{DGi} is the reactive power produced by ith DG.

C. INEQUALITY CONSTRAINTS

Voltage constraint: The bus voltages are required to be kept within the allowable range during the optimization process as expressed by (15)

$$V_{min} \le V_i \le V_{max} \tag{15}$$

where, V_{min} and V_{max} are the minimum and the maximum limits of the bus voltage, respectively.

Capacitor constraint: The reactive power compensation (QC) capacity of CB for a particular location is considered within the lower and upper limits as given in (16)

$$QC_{min} \le QC_i \le QC_{max} \tag{16}$$

where, QC_{min} and QC_{max} are the minimum and the maximum compensation capacity of CB, respectively.

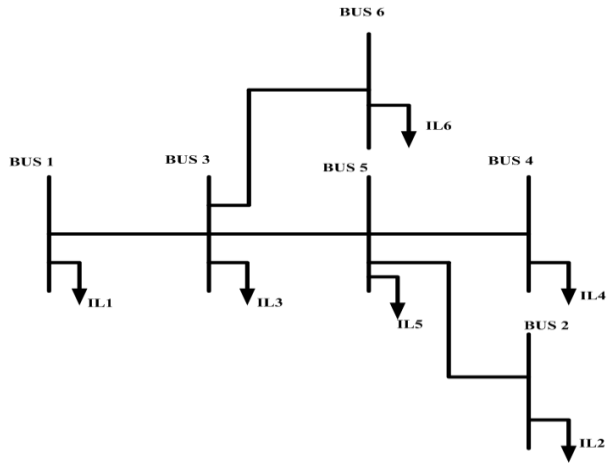

FIGURE 1. Single line diagram of the 6 bus RDS.

DG constraint: The DG's output is assumed to be within a limit and is expressed by (17)

$$P_{DG_{min}} \leq P_{DGi} \leq P_{DG_{max}} \tag{17}$$

where, $P_{DG_{min}}$ and $P_{DG_{max}}$ are the minimum and the maximum compensation capacity of DG, respectively.

Power factor constraint: The power factor of DG is also considered within a range and is given by (18)

$$PF_{min} \leq PF_i \leq PF_{max} \tag{18}$$

where, PF_i is the power factor of ith DG. PF_{min} and PF_{max} are the minimum and the maximum power factor limits, respectively.

Compensation capacity constraint: The total active and reactive power compensation capacities of DGs and CBs are considered within the maximum limit. For ith DG and CB, these are expressed by (19) and (20), respectively.

$$\sum_{i=1}^{NCB} QC_i \leq \sum_{i=1}^{NB} Q_{LD} \tag{19}$$

$$\sum_{i=1}^{NDG} P_{DGi} \leq 0.6 \times P_{LD} \tag{20}$$

Radiality constraint: In this work, an incident matrix (IM) of order $TNB \times TNB$ is created for checking the radiality of the system. Each element of IM is obtained using (21).

$$im_{i,j} = \begin{cases} 1 & \text{if node } i \text{ is directed} \\ & \text{towards node } j \\ 0 & \text{otherwise} \end{cases} \tag{21}$$

Except for the first column (considering slack bus node as 1), if each of the remaining columns of IM has one of the entries as '1' while the other components of each column have '0' value, the system is radial; otherwise, it is non-radial.

The constraints of the system during the optimization process employing QRSMA are handled based on the penalty factor method. When a specific variable goes out of the allowable limits (either of minimum and maximum limits), then the variable is multiplied by a large number and added to the objective function value as a penalty as shown in (22). This helps the variable to stay away from the infeasible solution space.

$$\text{Penalty} = \lambda_V + \lambda_{QC} + \lambda_{DG} + \lambda_{PF} \tag{22}$$

where, λ_V, λ_{QC}, λ_{DG} and λ_{PF} are the penalty factors of bus voltage, CB, DG and power factor constraints, respectively. These penalty factors are defined, respectively, in (23)-(26)

$$\lambda_V = PFW_V \times \left[\sum_{i=1}^{TNB} min(0, (V_i - V_{min})) + \sum_{i=1}^{TNB} min(0, (V_{max} - V_i)) \right] \tag{23}$$

$$\lambda_{QC} = PFW_{QC} \times \left[\sum_{i=1}^{NCB} min(0, (QC_i - QC_{min})) + \sum_{i=1}^{NCB} min(0, (QC_{max} - QC_i)) \right] \tag{24}$$

$$\lambda_{DG} = PFW_{P_{DG}} \times \left[\sum_{i=1}^{NDG} min(0, (P_{DG_i} - P_{DG_{min}})) + \sum_{i=1}^{NDG} min(0, (P_{DG_{max}} - P_{DG_i})) \right] \tag{25}$$

$$\lambda_{PF} = PFW_{PF} \times \left[\sum_{i=1}^{NDG} min(0, (PF_i - PF_{min})) + \sum_{i=1}^{NDG} min(0, (PF_{max} - PF_i)) \right] \tag{26}$$

where, PFW_V, PFW_{QC}, $PFW_{P_{DG}}$ and PFW_{PF} are the penalty function weights for bus voltage, CB, DG and power factor constraints having large positive values.

III. PROPOSED LOAD FLOW APPROACH

In the present work, a new branch current update-based modified backward forward load flow algorithm is proposed, which works well even with changing topology of RDS without depending upon the sequential numbering of nodes. This method is explained in detail by taking a small example of 6 bus reconfigured RDS (see Fig.1), where the connected buses

TABLE 2. Comparison of elapse time and number of iterations of load flow approaches.

Items	Proposed load flow approach			MATPOWER		
	69 bus	85 bus	118 bus	69 bus	85 bus	118 bus
Average Elapse Time (in sec)	0.0115	0.0226	0.0135	0.0578	0.0581	0.0577
Number of iterations	4	5	5	4	5	5

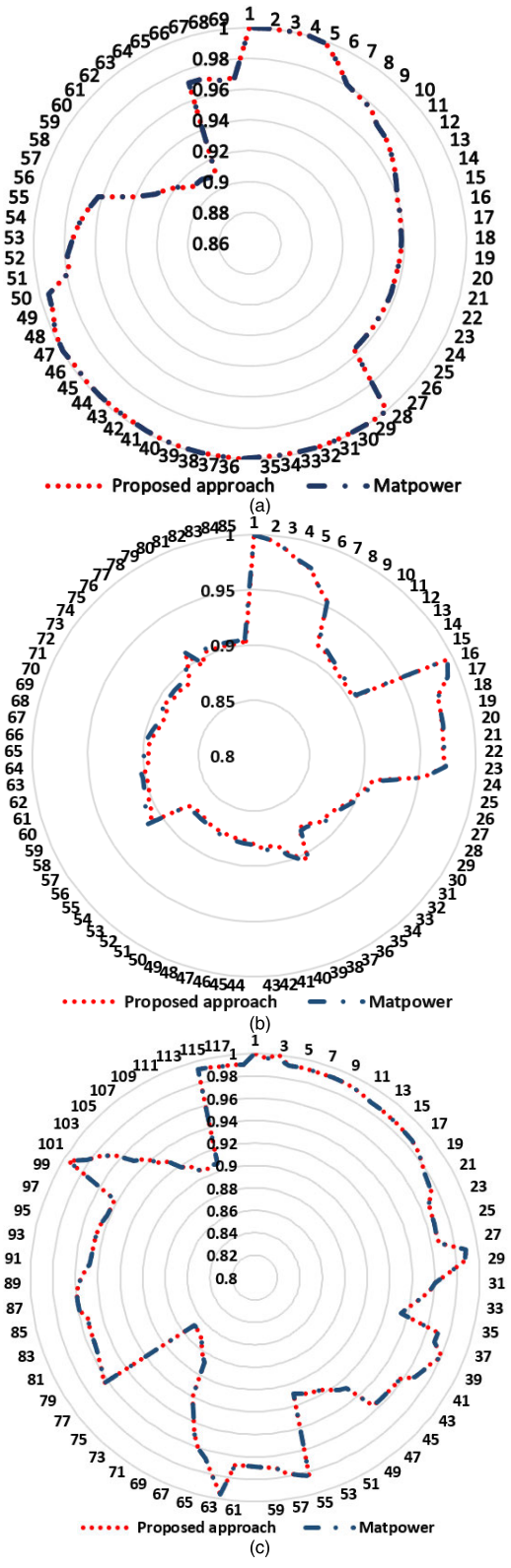

FIGURE 2. The comparison of bus voltages obtained for (a) 69 bus, (b) 85 bus, (c) 118 bus IEEE RDS.

are not in sequential order. In RDS, the slack bus is the starting bus connected to the grid and responsible for the power flow. In this model, bus number 1 is taken as the slack bus. Various ways can be used to locate the end buses. Once the starting and ending buses are known, the path connecting them may be found employing the graph theory approach. The paths obtained in terms of bus number for the RDS structure shown in Fig.1 are given as Path 1: [1 3 6], Path 2: [1 3 5 4], Path 3: [1 3 5 2].

In this method, branch currents are updated step by step. Initially, all the branch currents are considered to have zero value. Thereafter, the branch currents are updated by evaluating each of the connected paths one by one. The steps followed while updating the branch currents are

Step 1: Find the load current of each bus using (27)

$$IL_i = \left(\frac{P_i + jQ_i}{V_i}\right)^* \tag{27}$$

Step 2: For a particular path, start updating the branch current starting from the end bus to the slack bus.

Step 3: If the branch current is considered to be zero, then add the load current of the adjacent upper node with the subsequent branch currents, if any are present. For example, to update the branch current for path 1, the current of all the branches is first set to zero. Node 6 is an end node; therefore, no subsequent branch is present for it. Whereas, node 3 has a subsequent branch that connects it to node 6. So, the branch currents may be updated as follows

$$I_{36} = IL_6$$
$$I_{13} = IL_3 + I_{36}$$

Step 4: If the branch current is not zero, add the subsequent branch current to all the remaining branches along with their respective previous branch current values. For example, to update branch current for path 2, the current in the branches connected between node 5 and node 4 and between node 3 and node 5 are first set to zero, while the branch connected to node 1 and node 3 has some current value as it was updated in the previous step. So, the branch current for path 2 may be updated as follows.

$$I_{54} = IL_4$$
$$I_{35} = IL_5 + I_{54}$$
$$I_{13} = I_{35} + I_{13}$$

Similarly, for path 3, the branch current is updated as given below.

$$I_{52} = IL_2$$
$$I_{35} = I_{52} + I_{35}$$
$$I_{13} = I_{52} + I_{13}$$

Repeat the above steps until the current of all the branches gets updated.

In the proposed approach, the current summation method is adopted for obtaining bus voltages and other system parameters. The equations for the same is given by (28)-(30)

$$IL_i = \left(\frac{P_i + jQ_i}{V_i}\right)^* \tag{28}$$

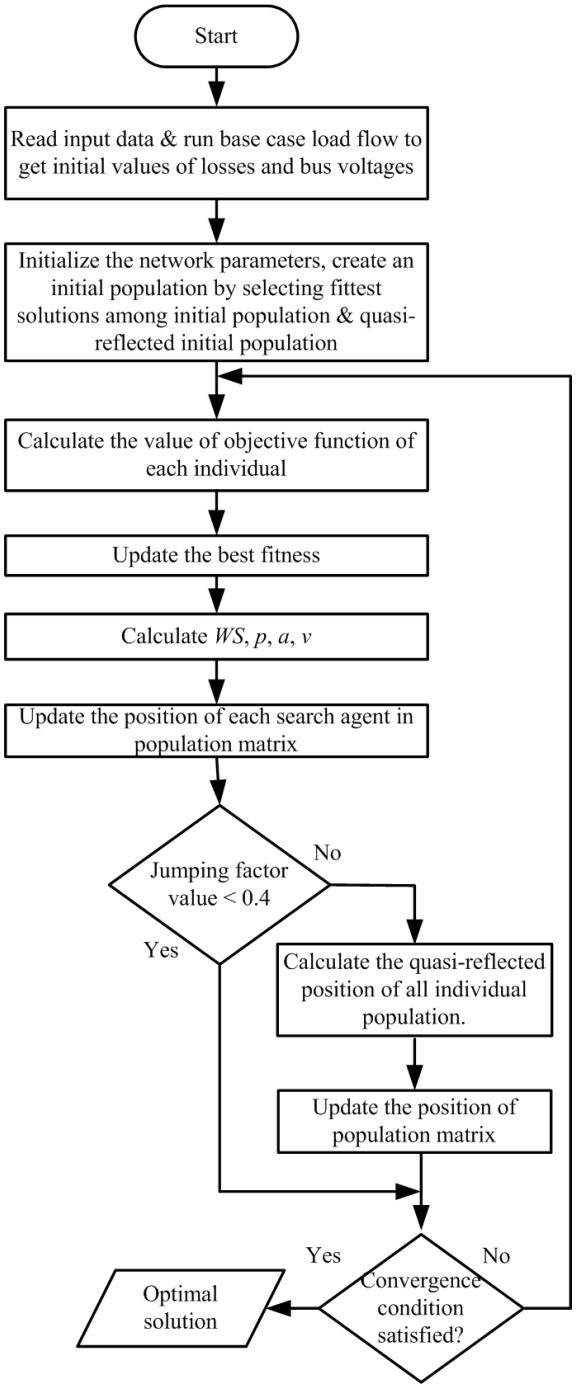

FIGURE 3. Flow chart of the proposed QRSMA.

$$I_{i-1,i} = I_{i,i+1} + IL_i \tag{29}$$

$$V_{i+1} = V_i - I_{i,i+1} \times (R_{i,i+1} + j \times X_{i,i+1}) \tag{30}$$

where, $R_{i,i+1}$ and $X_{i,i+1}$ are the resistance and the reactance of the branch connected between node i and $i+1$, respectively. The described approach is iteratively continued till the stopping criterion is met.

In order to validate the proposed load flow approach, its results are compared to those obtained using MATPOWER software for three different RDS configurations *i.e.*, 69 bus, 85 bus and 118 bus test systems. The backward forward sweep method with the current summation approach is selected in MATPOWER software to obtain the load flow solution. The tolerance limit is taken as 1e-4. For both approaches, the average elapsed time is obtained by executing the load flow module 50 times. The comparison of bus voltages obtained for various configurations using the proposed method and the MATPOWER is shown in Fig. 2. From Fig. 2, it may be observed that for each of the studied test systems, the bus voltages obtained utilizing both approaches are found to be nearly the same, which confirms the satisfactory performance of the proposed load flow technique. Table 2 reveals that the proposed load flow method takes less computational time than the compared software, making the presented approach more favorable. Low memory requirements, excellent computational efficiency and a simple structure are the key advantages of this technique, which may be applied to any RDS architecture without relying on the system node numbering.

TABLE 3. Value of different parameters used in calculating net annual cost of the system.

S.N.	Parameter description	Value
1	Average energy cost (K_e)	\$0.1/kWh
2	Purchase cost of capacitor (K_{cp})	\$3/kVAr
3	Installation cost of capacitor (K_{ci})	\$1000/location
4	Operation and maintenance cost of capacitor (K_{com})	\$300/location/year
5	Installation cost of DG (K_{dgin})	\$318000/MW
6	Operation and maintenance cost of DG (K_{dgom})	\$36/MWh
7	Cost per unit of energy not delivered (K_i)	\$4/kWh
8	Planning period (ny)	10 years
9	Inflation rate $(infr)$	9%
10	Interest rate $(intr)$	12.5%

IV. SMA AND QRSMA

This section delves into the specifics of SMA and the proposed QRSMA formulation.

A. SMA

SMA is developed by Li *et al.* and is based on the principle of food searching behavior of slime mould [33]. The slime mould is a eukaryote that is mainly found in frosty and moist areas. The slime mould surrounds the food source by its organic matter and digests it with the help of an enzyme. During the food searching process, the slime mould can access various food sources simultaneously by shaping into a venous-like network. When a vein moves towards a food source, the bio-oscillator generates propagating waves that boost its cytoplasm flow. When cytoplasmic flow increases, vein diameter expands, and when flow decreases, vein diameter contracts. This cytoplasmic flow acts as a feedback system that establishes the optimum

TABLE 4. Details of benchmark test functions.

Function Name	Expression	Range	Dimension	Min
Sphere	$f_1(n)=\sum_{i=1}^{d} n_i^2$	[-100,100]	30	0
Step	$f_2(n)=\sum_{i=1}^{d}\left(\lfloor n_i+0.5\rfloor\right)^2$	[-100,100]	30	0
Quartic	$f_3(n)=\sum_{i=1}^{d} i n_i^4+random(0,1)$	[-128,128]	30	0
Penalty 1	$f_4(n)=\frac{\pi}{d}\left\{10\sin(\pi y_i)+\sum_{i=1}^{d-1}(y_i-1)^2\left[1+10\sin^2(\pi y_{i+1})\right]+(y_d-1)^2\right\}$ $+\sum_{i=1}^{d} u(n_i,10,100,4)$ $y_i=1+\frac{n_i+1}{4}$ $u(n_i,a,k,m)=\begin{cases}k(n_i-a)^m & n_i>a\\ 0 & -a<n_i<a\\ k(-n_i-a)^m & n_i<-a\end{cases}$	[-50,50]	30	0
Penalty 2	$f_5(n)=0.1\left\{\begin{array}{l}\sin^2(3\pi n_i)+\sum_{i=1}^{d}(n_i-1)^2\left[1+\sin^2(3\pi n_{i+1})\right]\\ +(n_d-1)^2\left[1+\sin^2(2\pi n_d)\right]\end{array}\right\}$ $+\sum_{i=1}^{d} u(n_i,5,100,4)$	[-50,50]	30	0

TABLE 5. Summary of results obtained for different benchmark functions.

Algorithms		Functions				
		f_1	f_2	f_3	f_4	f_5
QRSMA (Proposed)	**best**	**0**	**1.5351e-04**	**8.7624e-05**	**7.8341e-08**	**7.0121e-08**
	mean	**1.1407e-282**	**0.0290**	**9.6523e-04**	**0.0038**	**0.0100**
	std	**0**	**0.0220**	**7.5791e-04**	**0.0054**	**0.0108**
SMA	best	3.2362e-185	0.0039	9.4989e-04	1.6116e-05	3.8181e-05
	mean	4.8296e-89	0.0699	0.0098	0.0050	0.0060
	std	1.8541e-88	0.1166	0.0068	0.0062	0.0077
SCA	best	0.0271	4.4124	50.1130	0.8855	2.7723
	mean	17.4545	16.0975	1.044e+06	3.3226e+04	1.5614e+05
	std	23.3433	17.2509	3.719e+06	1.6132e+05	5.4562e+05
SSA	best	2.9334e-08	3.8018e-08	0.0678	1.4930	0.0127
	mean	1.4189e-07	2.2453e-07	0.4924	6.8179	19.0387
	std	2.1432e-07	2.4821e-07	0.1959	3.0509	17.5475
WOA	best	1.2280e-88	0.1002	9.6238e-05	0.0042	0.1351
	mean	5.9470e-75	0.3691	0.0037	0.0216	0.6270
	std	2.0825e-74	0.2324	0.0034	0.0196	0.3014

pathway for the slime mould during foraging. Mathematically, imitation of its behavior is expressed as follows

$$Z_{itr+1}=\begin{cases} rand(0,1) & \\ \times (UB-LB)+LB & \text{if } rand(0,1)<h \\ Z_{itr}+r_b\times WS & \\ \times (Z_{itr}(A)-Z_{itr}(B)) & \text{if } v<p \\ r_c\times Z_{itr} & \text{if } v\geq p \end{cases} \tag{31}$$

where, Z_{itr} is the location of slime mould population for the iteration number *itr*, *LB* is the lower limit and *UB* is the upper limit of the searching agent, $Z_{itr}(A)$ and $Z_{itr}(B)$ are the two randomly selected locations from the total population, h is a constant taken as 0.1 for the current algorithm operation, r_b is a constant selected within the range $[-a, a]$, r_c varies linearly from 1 to 0 throughout the iteration, v is a random constant value in the range between [0, 1] and *WS* is the weight of slime mould. The value of p, *WS* and a are defined

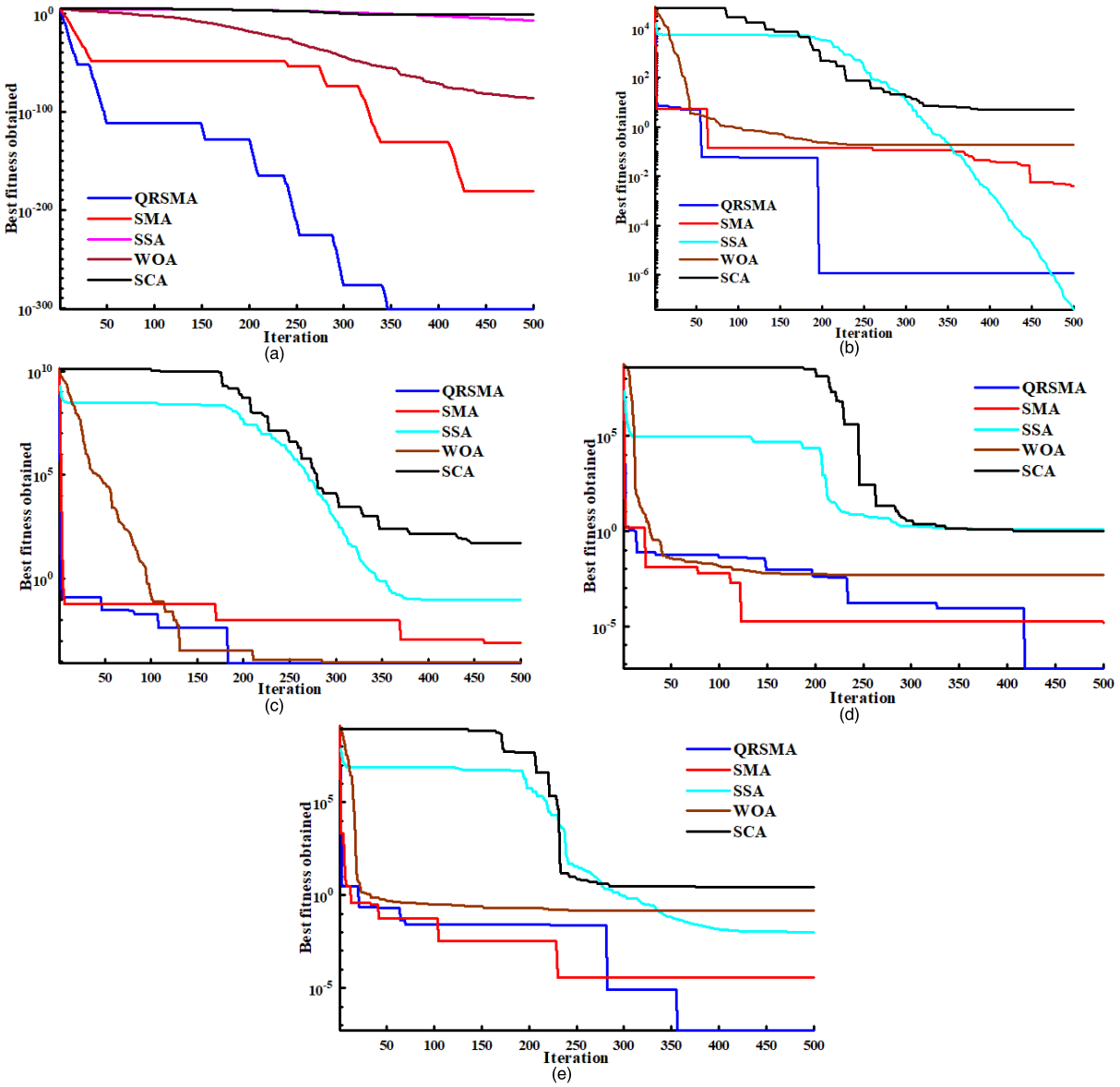

FIGURE 4. Comparative convergence curves obtained for different benchmark test functions (a) f_1, (b) f_2, (c) f_3, (d) f_4 and (e) f_5.

by (32)-(34), in order

$$p = \tanh(F(i) - BF) \tag{32}$$

$$a = arctanh\left(-\left(\frac{itr}{max\_itr}\right) + 1\right) \tag{33}$$

$$WS\ (Smell\_index(i)) = \begin{cases} 1 + v\ \log\left(\dfrac{CBF - F\ (i)}{CBF - CWF} + 1\right), & \text{condition} \\ 1 - v\ \log\left(\dfrac{CBF - F\ (i)}{CBF - CWF} + 1\right), & \text{else} \end{cases} \tag{34}$$

where, $F(i)$ is the fitness of the current agent and BF is the best fitness value, max_itr is the maximum number of iterations, CBF and CWF are the best and the worst fitness values of the current population, respectively. $Smell\_index$ signifies the sorted sequence of fitness values and it is expressed by (35).

$$Smell\_index = sort(F) \tag{35}$$

In (34), the condition implies that $F\ (i)$ lies in the first half of the sorted population. The internal composition of Z_{itr} for solving the ODGCBP issue along with OR is taken as per (36)

$$\begin{aligned} Z_{itr} = [&CB_{loc_1}, \ldots, CB_{loc_{NCB}}, CB_{size_1}, \ldots, CB_{size_{NCB}}, \\ &\times DG_{loc_1}, \ldots, DG_{loc_{NDG}}, DG_{size_1}, \ldots, DG_{size_{NDG}}, \\ &\times DG_{pf_1}, \ldots, DG_{pf_{NDG}}, SW_1, \ldots, SW_{nloop}] \end{aligned} \tag{36}$$

where, CB_{loc_n} and CB_{size_n} are the nth CB's location and size, respectively. DG_{loc_n}, DG_{size_n} and DG_{pf_n} are the nth DG's location, size and power factor, respectively. SW_n refers to the

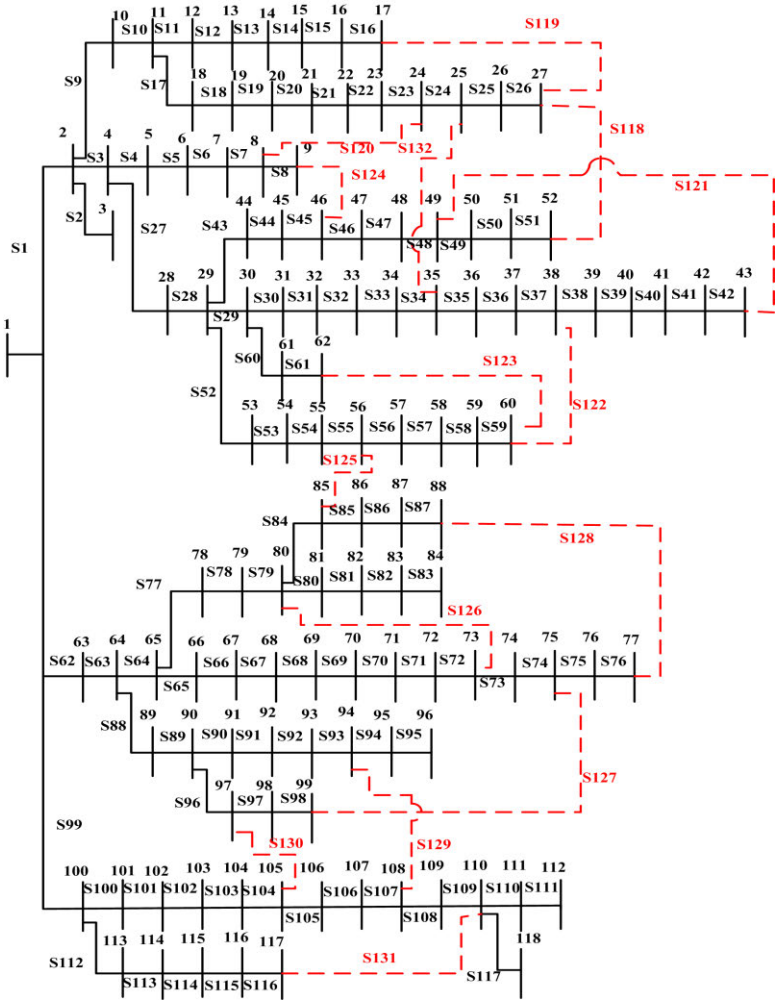

FIGURE 5. Single line diagram of standard IEEE 118 bus test system with reordered bus numbering.

open switch number or open branch number and *nloop* is the number of loops present in the base case system considering all the branches of RDS connected.

B. QRSMA

The opposition-based learning concept was first proposed by Tizhoosh [36], in which the current population and its opposite population are both considered simultaneously in order to obtain a better candidate solution. It has since been used by many researchers to improve the convergence characteristics of various optimization algorithms. In this method, the opposite point (OZ) of the current position or point (Z) is estimated with respect to the lower limit (ll) and upper limit (ul) as given in (37).

$$OZ = ul + ll - Z \tag{37}$$

After that, a quasi-opposition-based learning concept is developed, giving more efficient outcomes than the opposition-based concept [37]. In this method, the quasi-opposition point (QOZ) is estimated randomly in between the center point (CP) and the opposite point as given in (38) and (39).

$$CP = (ul + ll)/2 \tag{38}$$

$$QOZ = rand\,(CP, OZ) \tag{39}$$

Later, quasi-reflection-based population initialization is propounded by Ergezer *et al.* [32]. In [38], it has been mathematically illustrated that the convergence probability of the quasi-reflection-based approach is higher than the quasi-opposition-based approach. The quasi-reflection-point (QRZ) is the opposite point of quasi-opposition and is obtained as (40).

$$QRZ = rand\,(CP, Z) \tag{40}$$

The quasi-reflection idea is used in the proposed QRSMA during the population initialization as well as in the iterative phase. The steps involved in the initialization of the population in QRSMA are explained below.

Step 1: Initial population is randomly generated.

TABLE 6. Summary of results of IEEE 118 bus test system.

Items	Base Case	SCA	SSA	SMA	QRSMA
Capacitor location (size in kVAr)	-	63(1500) 64(1500) 65(1500) 67(1500) 107(1500) 111(1500) 114(1500)	48(1500) 55(1500) 84(1500) 85(1500)	22(1500) 37(1500) 43(1500) 81(1500) 84(1500) 106(1500)	**35(1500)** **55(1500)** **75(1500)** **79(1500)** **97(1500)** **103(1500)** **105(1500)**
DG location (size in kW, power factor)	-	54(1176,0.88) 58(809,0.88) 59(2000,0.88)	34(1095,0.85) 40(826,0.85) 54(1210,0.85) 63(1298,0.85) 64(1274,0.85) 70(986,0.85) 78(1165,0.85)	5(1829,0.93) 9(246,0.88) 28(135,0.97) 34(1355,0.86) 51(558,0.87) 62(1879,0.92) 67(1558,0.94) 107(1441,0.89) 110(1940,0.85)	**13(432,0.89)** **17(912,0.88)** **22(1898,0.93)** **53(1956,0.96)** **56(655,0.86)** **74(268,0.89)** **89(1671,0.93)** **96(38,0.95)** **107(1919,0.91)** **109(1706,0.98)**
Open switches	118, 119, 120, 121, 122, 123, 124, 125, 126, 127, 128, 129, 130, 131, 132	1, 12, 23, 24, 42, 44, 54, 70, 96, 97, 108, 118, 122, 128, 129	8, 15, 17, 28, 32, 46, 51, 52, 62, 71, 86, 98, 105, 120, 131	22, 27, 29, 30, 35, 40, 48, 62, 73, 79, 106, 112, 119, 124, 128	**7, 8, 12, 26, 27, 37, 41, 63, 64, 69, 74, 76, 107, 108, 123**
APLL (kW)	1297.248	401.913	531.478	329.041	**284.338**
RPLL (kVAr)	978.652	258.024	305.776	202.862	**170.240**
BV_{min} (p.u.)	0.869	0.941	0.971	0.949	**0.964**
CVD (p.u.)	3.306	0.285	0.0	0.152	**0.0**
ENS (kWh)	370573.301	136274.639	77991.603	131151.666	**51673.859**
RI (in %)	99.82	99.94	99.96	99.94	**99.98**
Net savings ($)	-	31220150.76	47965988.31	61030312.60	**65764437.94**
Elapse time (in sec)	-	615.43	633.59	660.17	**784.36**

Step 2: Quasi-reflection-based population is generated using (40).

Step 3: All of the populations are combined and sorted according to their fitness value. The best half of the population is chosen for the further algorithmic iterative process.

Following the initialization of the population, the iterative process of the algorithm starts. In every iteration, a generation jumping factor is calculated as a random value between 0 and 1. The generation jumping factor decides how often the quasi-reflection concept will be applied to the solutions, which increases the diversity among them. If the generation jumping factor value is greater than a predefined fixed value (user-defined), then the concept of quasi-reflection is implemented to generate an equal number of quasi-reflected solutions, same as the current population size using (40). At this point, the lower and the upper limits of a decision variable are defined as the lowest and the highest value of each variable in the current population, respectively. The flow chart of the proposed method is shown in Fig. 3.

V. RESULTS AND DISCUSSION

Firstly, the proposed QRSMA is tested on different multimodal and unimodal benchmark test functions. The yielded outputs under QRSMA are compared to those of recently reported algorithms to prove its effectiveness and superiority over the others. Thereafter, QRSMA is employed on IEEE 118 bus RDS to solve the problem of simultaneous ODGCBP and the OR. To demonstrate the efficacy of the proposed QRSMA, the obtained results are compared with that of other algorithms for the same test system. Afterward, QRSMA is utilized to solve the same issue of ODGCBP under variable loading scenarios, aiming to make the approach more realistic. In the proposed work, switchable capacitor bank is considered, as compensation capacity needed may vary with different loading conditions. The maximum limit for CB sizing is taken as 1500 kVAr for a single location with a step size of 50 kVAr. The DG's maximum limit is taken as 2 MW for a single location, whereas, the power factor (lagging) varied in between 0.85 to 1. The bus voltage constraint is considered within 0.9 p.u. to 1.05 p.u. The branch failure rate is taken as 0.1 for all the branches and the repair time is considered to be 10 hours. The maximum number of allowable locations for DG and CB is taken as 15 each. In the algorithm, the population size for solving the optimal placements of DG and CB along with OR is considered as 50 and the maximum iteration number as 100. The values of the different constants utilized for calculating system cost are given in Table 3. The purchase, installation and operation costs of CB are taken from [34], whereas, these costs for DG are taken from [35]. The cost per unit of energy and cost per unit of energy not supplied are taken from [15]. The proposed work is realized using MATLAB^R software. The system used for running the

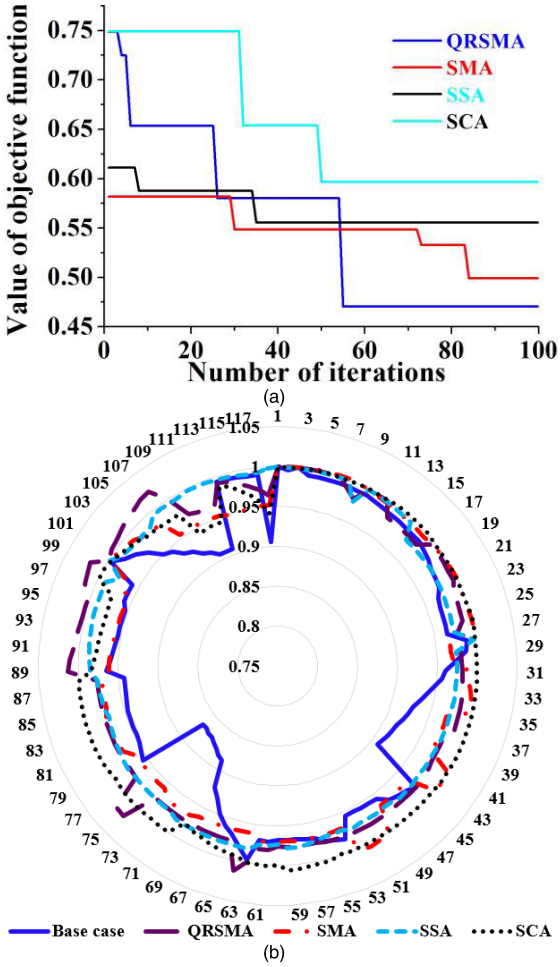

FIGURE 6. Results obtained for 118 bus test system (a) comparative convergence profiles (b) comparison of bus voltages.

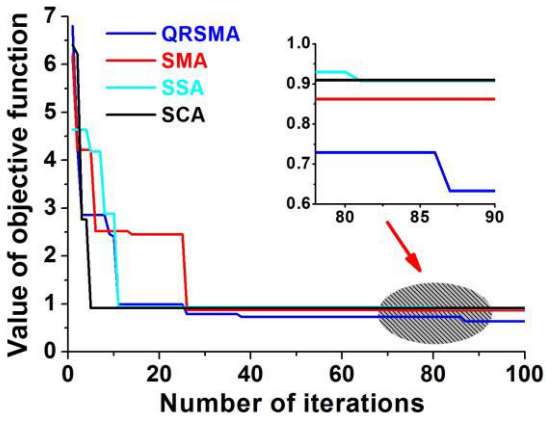

FIGURE 7. Results obtained for 118 bus test system comparative convergence profiles for variable loading condition.

algorithm consists of Intel core i7 processor of 8th generation with 8GB RAM. The important results are emphasized by highlighting them in bold in their respective tables and an entry of '−' in each table implies not applicable.

A. MATHEMATICAL BENCHMARK FUNCTIONS

The proposed QRSMA is tested on different unimodal and multimodal benchmark test functions to prove its superiority over the basic SMA and other reported algorithms. The detail on the considered test functions and their parameters are given in Table 4. The performance of different algorithms in terms of their mean, standard deviation and best value of obtained results are expressed in Table 5. The number of populations for the proposed QRSMA and other studied algorithms are taken as 30, while the number of iterations is set to 500 for all the benchmark functions. 30 different independent trial runs of each algorithm are performed to obtain the mean and standard deviation values of all functions. The values of different parameters of the studied algorithms are taken from [33]. From Table 5, it may be observed that QRSMA performs better than SMA and other algorithms in terms of mean value and standard deviation for each of the studied benchmark functions. The comparative convergence profiles obtained under each of the studied algorithms used for different benchmark functions are presented in Fig. 4. From Table 5 and Fig 4, it may be concluded that the proposed QRSMA offers superior and improved results over the other counterparts.

B. FIXED LOADING CONDITIONS

In the present work, QRSMA and other studied algorithms are applied to IEEE 118 bus radial distribution test system. The line data and load data of the studied RDS are taken from the work of [39]. The total base load demand of the system is (22709.71+j17040.97) kVA. The base values of the voltage and power considered for the simulation work are 11 kV and 100 MVA, respectively. The single line diagram of 118 bus system is shown in Fig. 5 with their sectionalized and tie-line switches' positions clearly indicated. Before applying any compensation techniques, using the proposed modified load flow approach, the active and reactive power line losses of the system under base load are obtained as 1297.248 kW and 978.652 kVAr, respectively. All the studied algorithms aim to optimize the location, size, number and power factor of DGs and CBs and, simultaneously, aim to achieve OR of RDS structure by minimizing line losses, bus voltage deviations and total system cost and maximizing system reliability. The other algorithms studied along with the proposed QRSMA are SMA, SCA and SSA. The obtained simulation results consisting of optimal location and size of DGs and CBs along with OR of RDS are shown in Table 6. The comparative convergence and bus voltage magnitude profiles yielded using different algorithms are displayed in Fig. 6. From Table 6, it may be observed that using QRSMA, the total reactive power compensation capacity of 10500 kVAr is obtained for 7 different optimal locations found for CB placement, whereas, the total active power compensation of 11455 kW is obtained for optimal DG placement at 10 different locations. The cost of energy saved by deploying the QRSMA based obtained DG and CB sizes with their respective power factors at the optimal locations in an

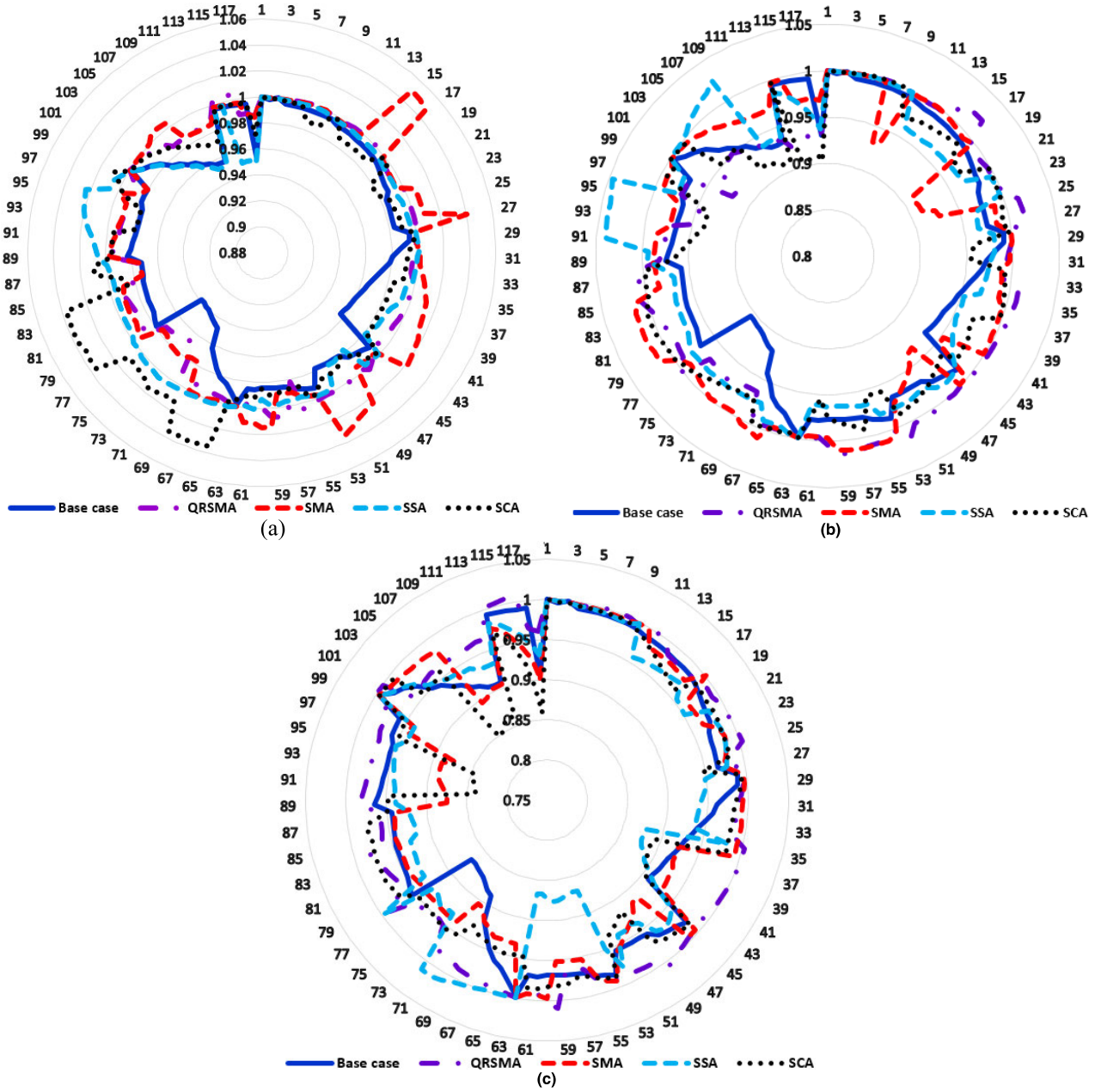

FIGURE 8. Comparison of bus voltages for 118 bus test system for variable loading conditions (a) LF = 1, (b) LF = 0.75, (c) LF = 0.5.

optimal reconfigured network is found as \$102,666,386.8. The purchase and operation and maintenance costs of DGs are obtained as \$6,360,000 and \$30,485,726.79, respectively. Whereas, the purchase cost of CBs is obtained as \$31,500.0 and the sum of installation and operation and maintenance costs of CBs is obtained as \$24,722.06. This results in a total net profit of \$65,764,437.94 utilizing the proposed approach. Fig 6 shows that the bus voltages obtained, after deploying the yielded optimal results from all the algorithms, are well within the allowable voltage limits. The *APLL* and the *RPLL* values are obtained as 284.338 kW and 170.240 kVAR, respectively, employing QRSMA. The value of ENS is reduced from 370573.301 kWh to 51673.859 kWh post compensation. The minimum bus voltage is improved to a value of 0.964 p.u. The result obtained through SCA produces a minimal amount of installation and operation cost of DGs and CBs. But, due to the less amount of offered active and reactive power compensation, the system's loss reduction is found to be less, which in return results in low revenue collection from energy saving. Therefore, the overall profit of the system is obtained as minimal. It may be observed from Table 6 that with the increase in the amount of compensation, the loss reduction increases and the minimum bus voltage improves as well. Employing SSA results in selecting more

TABLE 7. Optimal location, size and number of DGs and CBs and location of open switches for IEEE 118 bus RDS obtained under variable loading conditions using QRSMA.

Load Factor/ Compensation	DG location (size in kW, power factor)	Capacitor location (size in kVAr)	Open switches
1	6(1165,0.97), 25(1603,0.92), 38(1092,0.99), 46(243,0.96), 48(1077,0.88), 55(445,0.93), 70(869,0.95), 84(1722,0.98), 90(1420,0.95), 93(1025,0.93), 95(263,0.91), 111(1450,0.89), 115(976,0.92)	3(300), 13(1100), 23(700), 39(1350), 49(1500), 56(150), 59(1200), 61(1200), 64(1250), 68(800), 80(50), 83(550), 90(400), 107(750), 117(950)	6, 13, 20, 25, 34, 48, 58, 72, 75, 78, 101, 105, 116, 123, 127
0.75	6(530,1), 17(893,0.91), 25(366,0.94), 38(869,0.94), 46(1067,0.93), 48(359,0.88), 55(1178,0.95), 57(777,0.97), 84(1048,0.88), 90(1021,0.87), 93(369,0.99), 95(831,0.98), 111(445,0.91), 115(367,0.91)	3(200), 13(700), 23(850), 39(900), 49(1200), 56(650), 59(1050), 61(250), 64(800), 68(1100), 80(1050), 83(100), 90(950), 107(150), 117(1300)	6, 14, 20, 24, 33, 51, 59, 61, 68, 74, 76, 84, 93, 99, 101
0.5	17(207,0.93), 25(291,0.93), 38(509,0.93), 46(593,0.98), 48(270,0.89), 55(744,0.95), 57(434,1), 70(462,0.96), 84(457,0.92), 90(950,1), 93(209,0.98), 95(215,0.91), 111(647,0.90), 115(674,0.92)	3(650), 13(400), 23(750), 39(400), 49(700), 56(350), 59(950), 61(800), 64(400), 68(200), 80(700), 83(300), 90(300), 107(750), 117(800)	13, 21, 33, 45, 46, 55, 56, 61, 71, 89, 105, 115, 121, 126, 127
Fixed Compensation	25(291), 38(509), 46(243), 48(270), 55(445), 84(457), 90(950), 93(209), 95(215), 111(445), 115(367)	3(200), 13(400), 23(700), 39(400), 49(700), 56(150), 59(950), 61(250), 64(400), 68(200), 80(50), 83(100), 90(300), 107(150), 117(800)	
Variable Compensation	6((1165), 17(893), 25(1312), 38(583), 46(824), 48(807), 55(733), 57(777), 70(869), 84(1265), 90(470), 93(816), 95(616), 111(1005), 115(609)	3(450), 13(700), 23(150), 39(950), 49(800), 56(500), 59(250), 61(950), 64(850), 68(900), 80(1000), 83(450), 90(650), 107(600), 117(500)	

TABLE 8. Optimal location, size and number of DGs and CBs and location of open switches for IEEE 118 bus RDS obtained under variable loading conditions using SMA.

Load Factor/ Compensation	DG location (size in kW, power factor)	Capacitor location (size in kVAr)	Open switches
1	15(407,0.89), 16(345,1), 25(567,0.97), 29(1321,0.94), 40(1328,0.90), 54(1959,0.87), 60(853,0.97), 67(1399,0.99), 80(297,0.87), 81(602,0.87), 85(323,0.88), 93(1493,0.97), 105(569,0.98)	8(1150), 9(200), 15(450), 18(900), 31(700), 33(1000), 35(1150), 36(1350), 67(150), 98(1450), 104(50), 110(950), 112(1050), 117(300)	11, 18, 34, 36, 45, 59, 63, 71, 75, 88, 97, 107, 122, 124, 130
0.75	15(982,0.87), 25(787,0.87), 40(1239,0.94), 54(1612,0.92), 60(576,0.94), 67(382,0.89), 80(1300,0.89), 81(1269,0.98), 85(838,0.92), 93(235,0.93), 105(803,0.90)	8(1250), 9(500), 15(150), 18(300), 31(300), 33(650), 35(1100), 36(200), 67(750), 98(550), 104(650), 110(950), 112(1150), 117(1100)	7, 18, 24, 31, 35, 41, 45, 59, 66, 78, 85, 92, 96, 114, 130
0.5	16(1035,0.86), 29(330,0.91), 40(1011,0.99), 54(301,0.89), 60(984,0.98), 67(481,0.96), 80(220,0.90), 81(694,0.97), 105(1338,0.86)	8(650), 9(400), 15(350), 18(500), 31(50), 33(200), 35(300), 36(1000), 67(250), 98(950), 104(950), 110(50), 112(1100), 117(1100)	14, 22, 26, 47, 58, 60, 69, 84, 85, 97, 104, 107, 116, 120, 124
Fixed Compensation	40(1011), 54(301), 60(576), 67(382), 80(220), 81(602), 105(569)	8(650), 9(200), 15(150), 18(300), 31(50), 33(200), 35(300), 36(200), 67(150), 98(550), 104(50), 110(50), 112(1050), 117(300)	
Variable Compensation	15(982), 16(1035), 25(787), 29(1321), 40(317), 54(1658), 60(408), 67(1017), 80(1080), 81(667), 85(838), 93(1493), 105(769)	8(500), 9(300), 15(300), 18(600), 31(650), 33(800), 35(850), 36(1150), 67(600), 98(900), 104(900), 110(900), 112(100), 117(800)	

DGs with minimum allowable power factor value (0.85 lag), which helps compensate both active and reactive powers at the installed location. Because of this, the algorithm chooses less number of CBs for reactive power compensation. Referring Table 6, QRSMA outperforms the studied SMA, SSA and SCA. The *APLL* and *RPLL* values obtained using QRSMA are the minimum, while the obtained net profit is the maximum among all studied algorithms, which shows the dominance of the proposed algorithm in solving the studied problem. However, the minimum bus voltages found under

TABLE 9. Optimal location, size and number of DGs and CBs and location of open switches for IEEE 118 bus RDS obtained under variable loading conditions using SSA.

Load Factor/ Compensation	DG location (size in kW, power factor)	Capacitor location (size in kVAr)	Open switches
1	2(989,0.89), 5(1636,0.86), 50(1550,0.89), 71(1812,0.97), 73(406,0.95), 75(1640,0.90), 93(638,0.86), 96(852,0.90)	4(600), 6(500), 21(200), 29(1150), 43(1100), 47(1450), 49(1400), 52(600), 58(400), 59(950), 61(600), 66(300), 72(400), 77(1050), 96(250)	10, 20, 27, 34, 35, 51, 53, 60, 72, 78, 84, 88, 109, 125, 129
0.75	2(1184,0.93), 5(1111,0.98), 30(1467,0.88), 50(1033,0.91), 71(698,0.87), 73(473,0.96), 75(1070,0.96), 93(1307,0.91), 94(838,0.91), 96(1029,0.89)	4(750), 6(500), 21(1450), 29(1050), 43(950), 47(250), 49(750), 58(200), 59(800), 61(800), 72(900), 77(750), 96(600)	10, 21, 24, 27, 35, 54, 60, 67, 87, 90, 96, 108, 118, 122, 130
0.5	5(359,0.90), 30(1912,0.87), 71(312,0.95), 73(1211,0.89), 93(961,0.92), 94(328,0.92), 96(635,0.99)	4(1000), 6(150), 21(200), 29(1050), 43(100), 47(200), 49(700), 52(750), 58(200), 59(500), 61(650), 66(500), 72(1000), 77(900), 96(500)	23, 34, 37, 46, 50, 57, 65, 76, 78, 98, 114, 120, 124, 129, 130
Fixed Compensation	5(359), 71(312), 73(406), 93(638), 96(635)	4(600), 6(150), 21(200), 29(1050), 43(100), 47(200), 49(700), 58(200), 59(500), 61(600), 72(400), 77(750), 96(250)	
Variable Compensation	2(1184), 5(1277), 30(1912), 50(1550), 71(1500), 73(805), 75(1640), 93(669), 94(838), 96(394)	4(400), 6(350), 21(1250), 29(100), 43(1000), 47(1250), 49(700), 52(750), 58(200), 59(450), 61(200), 66(500), 72(600), 77(300), 96(350)	

TABLE 10. Optimal location, size and number of DGs and CBs and location of open switches for IEEE 118 bus RDS obtained under variable loading conditions using SCA.

Load Factor/ Compensation	DG location (size in kW, power factor)	Capacitor location (size in kVAr)	Open switches
1	4(1093,0.90), 7(654,0.96), 26(486,0.92), 50(200,0.92), 78(1453,0.85), 81(1646,0.97), 86(1041,0.91), 91(230,0.87), 99(761,0.94), 106(1246,0.86), 116(491,0.92)	22(1000), 24(350), 37(1000), 62(850), 67(800), 79(750), 86(1050), 94(450), 95(300), 98(250), 101(650)	23, 26, 36, 48, 57, 62, 70, 78, 87, 90, 102, 106, 120, 122, 124
0.75	4(538,0.88), 7(862,0.87), 26(1404,0.93), 47(1691,0.87), 50(918,0.99), 78(403,0.98), 80(612,0.85), 81(1052,1), 82(563, 0.91), 86(1512,0.98), 99(484,0.89)	22(700), 24(950), 37(1400), 62(800), 64(100), 67(1200), 79(400), 86(1400), 94(1400), 95(400), 98(1500)	9, 20, 28, 31, 37, 39, 55, 61, 68, 97, 102, 106, 113, 124, 126
0.5	4(793,0.85), 7(521,1), 26(915,0.88), 47(312,0.93), 50(377,0.88), 80(951,0.93), 81(1044,0.95), 91(376,0.92), 99(954,0.88)	22(100), 24(300), 37(250), 62(650), 64(700), 67(800), 79(1050), 86(1450), 94(300), 95(650), 98(150)	6, 11, 19, 34, 45, 48, 54, 62, 64, 69, 84, 86, 92, 131, 132
Fixed Compensation	4(538), 7(521), 26(486), 50(200), 81(1044), 99(484)	22(100), 24(300), 37(250), 62(650), 67(800), 79(400), 86(1050), 94(300), 95(300), 98(150)	
Variable Compensation	4(555), 7(341), 26(918), 47(1691), 50(718), 78(1453), 80(951), 81(602), 82(563), 86(1512), 91(376), 99(470), 106(1246), 116(491)	22(900), 24(650), 37(1150), 62(200), 64(700), 67(400), 79(650), 86(400), 94(1100), 95(350), 98(1350), 101(650)	

the proposed approach are almost comparable to those of other algorithms and are satisfactorily inside the permissible limits. The CVD value is found near zero under each of the studied algorithms, which shows the efficacy of the adopted approach in solving the chosen distribution system issue.

C. VARIABLE LOADING CONDITIONS

The fixed loading scenario is not a viable approach, as in the real world, the load demands vary with time. Moreover, the results obtained for a particular loading condition may not be relevant technically and economically for other loading scenarios. For example, during a higher load demand scenario, the number of locations and size of DGs and CBs required are more. The above scenario may not appear to be economical during light load conditions (as the power compensation required for lower load levels are less) causing additional installation and maintenance costs. This may lead to non-profitable solutions depending upon the duration of low load demand scenario. On the other hand, the amount of compensation obtained for low demand scenario when used for higher load demand operation, may lead to problems like higher line losses, off-limit bus voltages, and reverse

TABLE 11. Summary and results of IEEE 118 bus test system obtained under variable loading conditions.

Items	QRSMA			SMA		
	Load Factor			Load Factor		
	1	0.75	0.5	1	0.75	0.5
$APLL_b$ (in kW)	1297.2	696.9	297.0	1297.2	696.9	297.0
$APLL_a$ (in kW)	448.098	354.054	115.487	910.3	602.4	204.4
% reduction in $APLL$	65.46	49.20	61.12	29.82	13.56	31.18
$RPLL_b$ (in kVAr)	978.652	527.222	225.218	978.652	527.222	225.218
$RPLL_a$ (in kVAr)	312.224	233.534	75.612	541.320	383.345	127.282
% reduction in $RPLL$	68.10	55.70	66.43	44.69	27.29	43.48
$BV_{\min b}$ (in p.u.)	0.869	0.905	0.939	0.869	0.905	0.939
BV_{min_a} (in p.u.)	0.949	0.920	0.967	0.974	0.911	0.874
CVD_b (in p.u.)	3.306	1.710	0.466	3.306	1.710	0.466
CVD_a (in p.u.)	0.101	1.275	0.0	4.399	0.815	0
ENS_b (in kWh)	123524.43	68128.79	29735.09	123524.43	68128.79	29735.09
ENS_a (in kWh)	72269.6	40944.4	17786.1	85772.96	51764.00	20336.24
RI_b (in %)	99.94	99.96	99.97	99.94	99.96	99.97
RI_a (in %)	99.97	99.97	99.98	99.96	99.97	99.98
Total net profit (in $)	Energy purchase cost saving -Total DG and CB installation, operation and maintenance costs = 84,730,556.096-55,268,115.52 = 29,462,440.576			Energy purchase cost saving -Total DG and CB installation, operation and maintenance costs =75,331,821.70-51,118,160.35=24,213,661.35		

Items	SSA			SCA		
	Load Factor			Load Factor		
	1	0.75	0.5	1	0.75	0.5
$APLL_b$ (in kW)	1297.2	696.9	297.0	1297.2	696.9	297.0
$APLL_a$ (in kW)	1244.0	591.8	290.3	1106.8	607.9	258.5
% reduction in $APLL$	4.10	15.08	2.26	14.68	12.77	12.96
$RPLL_b$ (in kVAr)	978.652	527.222	225.218	978.652	527.222	225.218
$RPLL_a$ (in kVAr)	819.522	374.345	187.175	194.958	405.514	194.958
% reduction in $RPLL$	16.26	29.00	16.89	80.08	23.08	13.44
$BV_{\min b}$ (in p.u.)	0.869	0.905	0.939	0.869	0.905	0.939
BV_{min_a} (in p.u.)	0.951	0.937	0.867	0.839	0.906	0.972
CVD_b (in p.u.)	3.306	1.710	0.466	3.306	1.710	0.466
CVD_a (in p.u.)	4.974	0.308	0	4.040	1.284	0
ENS_b (in kWh)	123524.43	68128.79	29735.09	123524.43	68128.79	29735.09
ENS_a (in kWh)	128470.0	62620.42	24895.10	103291.2	52308.8	21541.7
RI_b (in %)	99.94	99.96	99.97	99.94	99.96	99.97
RI_a (in %)	99.94	99.96	99.98	99.95	99.97	99.98
Total net profit (in $)	Energy purchase cost saving -Total DG and CB installation, operation and maintenance costs = 65,768,403.00-44,126,106.151= 21,642,296.849			Energy purchase cost saving -Total DG and CB installation, operation and maintenance costs = 67,361,659.972 - 49,330,797.091 = 18,030,862.881		

power flows. Apart from the above, the optimal configuration of RDS may also vary with variable loading situations. So, to address the above-mentioned issues, three different loading scenarios (i.e., full, medium and light load conditions) have been taken for further investigation as considered in [34]. The amount of compensation realized employing DGs and CBs for different loading states in an optimized RDS topology is found by simultaneously considering the cost-benefit

analysis of the proposed approach. The base load demand is multiplied by a factor of 1, 0.75, and 0.5, respectively, to realize full, medium, and light load scenarios. The respective load factor durations are taken as 40%, 35% and 25% of the total project duration.

The optimal solution for each load factor (or loading scenario) is first obtained independently. Thereafter, combining them, a final technically feasible solution is found. But, as the obtained solution may vary for each loading condition, the optimal locations of DGs and CBs may also differ from one solution to the next. This may increase the combined number of locations, resulting in high installation and operation costs for deployed DGs and CBs. So, to avoid such problems, in this work, simultaneous ODGCBP along with OR of RDS has been done considering all the load factors at the same time. The adopted objective function is calculated using the average value of the power loss and bus voltage deviation parameters found considering each loading factor at a time. After that, the total system's cost is estimated taking into account of the combined locations of DGs and CBs obtained under each of the three loading scenarios.

Fig. 7 depicts the comparative convergence profiles obtained using the investigated optimization approaches. Fig. 8 compares the bus voltages obtained using the adopted methodology under various loading scenarios. The optimal locations and sizes of DGs and CBs along with OR obtained under the studied algorithms are presented in Tables 7-Table 10. It can be seen from Fig. 7 that the convergence profiles appear to be converged close to each other. Due to the addition of penalty function values, the objective function value is fairly high (about 6 to 7, as seen in Fig. 7) during the initial phase of iterations. This occurs primarily as a result of constraint violations in the solutions during the initial iteration phase. On the other hand, all of the analyzed algorithms' objective function values are penalty-free and well within acceptable limits during the final optimization phase. As a result, in comparison to their high initial values, all of the algorithms' final convergence values appear to be reasonably close to each other. However, as shown in the zoomed-in view of Fig. 7, it is observed that the QRSMA performs better than its competitors. The simulation outcomes are presented in a comparative format in Table 11. From Tables 7-10, it may be observed that the installation location of DGs and CBs for all three loading scenarios are nearly identical. So, the total installation cost will be lower as the combined number of locations will be lesser. In the presence of QRSMA based ODGCBP and OR, for full, medium, and light load scenarios, active power line losses are decreased by 65.46 percent, 49.20 percent, and 61.12 percent, respectively, and reactive power line losses are reduced by 68.10 percent, 55.70 percent, and 66.43 percent, respectively, in comparison to that of uncompensated base case loading of RDS. In this case (i.e., employing QRSMA), the combined energy saving cost considering the full, medium and light load conditions together is obtained as \$84,730,556.096. The number of optimal locations for DGs and CBs are found as 15 each. Their respective total sizes are 17,145 kW and 15,450 kVAr. The purchase and operation and maintenance costs for DGs and CBs are, respectively, \$55,168,789.68 and \$99,325.84. Finally, the total profit is found as \$29,462,440.576. Similarly, after the compensation, the percentage reduction in APLL and RPLL obtained using SMA, SSA and SCA are shown in Table 11. The net saving found employing SMA, SSA and SCA based ODGCBP and OR of RDS are \$24,213,661.35, \$21,642,296.849 and \$18,030,862.881, respectively. From the above given results, it is inferred that the QRSMA based obtained ODGCBP and OR of RDS outperforms all other algorithms in terms of bus voltages profile improvement, reduction in active and reactive power losses and the net annual profit obtained. This demonstrates the efficacy and superiority of QRSMA over the others.

VI. CONCLUSION

In the present work, QRSMA, an improved version of SMA is proposed for the first time. QRSMA's superiority over SMA and other published algorithms is examined and verified using several unimodal and multimodal benchmark test functions. A new branch current update-based modified load flow approach is proposed. It is suitable for any RDS topology and capable of producing desirable results. The proposed modified load flow approach is independent of the sequential bus numbering scheme and does not require matrix calculations. This helps fasten its convergence speed in finding solutions for larger RDS. The optimal sizing and placement of DGs and CBs along with OR are solved successfully for 118 bus RDS employing the proposed QRSMA and the modified load flow method. The formulated objective function comprises line losses, cumulative voltage deviation, reliability index, and total system cost for producing a realistic solution subject to various equality and inequality constraints. Results found employing QRSMA are compared to that of the other established algorithms. The number, location and size of DGs (considering variable power factor value) and CBs are optimized simultaneously along with another objective of finding OR for the studied RDS. The performance of the proposed algorithm under variable loading scenarios are evaluated to make the approach more practical. From the obtained results, it may be concluded that QRSMA offers better solutions and convergence characteristics in comparison to other studied algorithms. The essence of the conclusion may be stated as

- A new improved algorithm called QRSMA is proposed for the first time.
- An efficient modified load flow algorithm is proposed, which does not require sequential bus numbering of RDS for finding a solution.
- Simultaneous optimal DG and CB placement with OR of RDS is solved under both fixed and variable loading conditions considering line losses, cumulative bus voltage deviation, reliability index, and total system cost based defined objective function.

- A cost-benefit analysis of the proposed method is also carried out.

Other technological, environmental, and economic aspects may be taken into account in the future, together with the use of more complex optimization techniques, to create a more successful solution for ODGCBP and OR of RDS. The concept of Pareto optimality can also be used to deal with goals that are mutually exclusive. The impact of uncertainty in the load demand and the generation on the performance of the proposed approach may be also explored.

REFERENCES

[1] A. A. A. El-Ela, R. A. El-Sehiemy, and A. S. Abbas, "Optimal placement and sizing of distributed generation and capacitor banks in distribution systems using water cycle algorithm," *IEEE Syst. J.*, vol. 12, no. 4, pp. 3629–3636, Dec. 2018.

[2] A. M. Shaheen and R. A. El-Sehiemy, "Optimal coordinated allocation of distributed generation units/capacitor banks/voltage regulators by EGWA," *IEEE Syst. J.*, vol. 15, no. 1, pp. 257–264, Mar. 2021.

[3] K. Muthukumar and S. Jayalalitha, "Integrated approach of network reconfiguration with distributed generation and shunt capacitors placement for power loss minimization in radial distribution networks," *Appl. Soft Comput.*, vol. 52, pp. 1262–1284, Mar. 2017.

[4] S. R. Biswal and G. Shankar, "Simultaneous optimal allocation and sizing of DGs and capacitors in radial distribution systems using SPEA2 considering load uncertainty," *IET Gener., Transmiss. Distrib.*, vol. 14, no. 3, pp. 494–505, Feb. 2020.

[5] M. E. Baran and F. F. Wu, "Optimal capacitor placement on radial distribution systems," *IEEE Trans. Power Del.*, vol. 4, no. 1, pp. 725–734, Jan. 1989.

[6] S. K. Goswami and S. K. Basu, "A new algorithm for the reconfiguration of distribution feeders for loss minimization," *IEEE Trans. Power Del.*, vol. 7, no. 3, pp. 1484–1491, Jul. 1992.

[7] D. Das, H. S. Nagi, and D. P. Kothari, "Novel method for solving radial distribution networks," *IEE Gener., Transmiss. Distrib.*, vol. 141, no. 4, pp. 291–298, Jul. 1994.

[8] J.-H. Teng, "A direct approach for distribution system load flow solutions," *IEEE Trans. Power Del.*, vol. 18, no. 3, pp. 882–887, Jul. 2003.

[9] A. M. Elsayed, M. M. Mishref, and S. M. Farrag, "Optimal allocation and control of fixed and switched capacitor banks on distribution systems using grasshopper optimisation algorithm with power loss sensitivity and rough set theory," *IET Gener., Transmiss. Distrib.*, vol. 13, no. 17, pp. 3863–3878, Sep. 2019.

[10] A. Jafari, H. Ganjeh Ganjehlou, T. Khalili, B. Mohammadi-Ivatloo, A. Bidram, and P. Siano, "A two-loop hybrid method for optimal placement and scheduling of switched capacitors in distribution networks," *IEEE Access*, vol. 8, pp. 38892–38906, 2020.

[11] P. D. Huy, V. K. Ramachandaramurthy, J. Y. Yong, K. M. Tan, and J. B. Ekanayake, "Optimal placement, sizing and power factor of distributed generation: A comprehensive study spanning from the planning stage to the operation stage," *Energy*, vol. 195, Mar. 2020, Art. no. 117011.

[12] M. D. Hraiz, J. A. M. Garcia, R. J. Castaneda, and H. Muhsen, "Optimal PV size and location to reduce active power losses while achieving very high penetration level with improvement in voltage profile using modified Jaya algorithm," *IEEE J. Photovolt.*, vol. 10, no. 4, pp. 1166–1174, Jul. 2020.

[13] K. Mahmoud and M. Lehtonen, "Comprehensive analytical expressions for assessing and maximizing technical benefits of photovoltaics to distribution systems," *IEEE Trans. Smart Grid*, early access, Jul. 15, 2021, doi: 10.1109/TSG.2021.3097508.

[14] A. Selim, S. Kamel, A. S. Alghamdi, and F. Jurado, "Optimal placement of DGs in distribution system using an improved Harris Hawks optimizer based on single- and multi-objective approaches," *IEEE Access*, vol. 8, pp. 52815–52829, 2020.

[15] A. K. Bohre, G. Agnihotri, and M. Dubey, "Optimal sizing and sitting of DG with load models using soft computing techniques in practical distribution system," *IET Gener., Transmiss. Distrib.*, vol. 10, no. 11, pp. 2606–2621, Aug. 2016.

[16] A. Waqar, U. Subramaniam, K. Farzana, R. M. Elavarasan, H. U. R. Habib, M. Zahid, and E. Hossain, "Analysis of optimal deployment of several DGs in distribution networks using plant propagation algorithm," *IEEE Access*, vol. 8, pp. 175546–175562, 2020.

[17] X. Xu, J. Li, Y. Xu, Z. Xu, and C. S. Lai, "A two-stage game-theoretic method for residential PV panels planning considering energy sharing mechanism," *IEEE Trans. Power Syst.*, vol. 35, no. 5, pp. 3562–3573, Sep. 2020.

[18] S. Das, D. Das, and A. Patra, "Operation of distribution network with optimal placement and sizing of dispatchable DGs and shunt capacitors," *Renew. Sustain. Energy Rev.*, vol. 113, Oct. 2019, Art. no. 109219.

[19] K. Mahmoud and M. Lehtonen, "Simultaneous allocation of multi-type distributed generations and capacitors using generic analytical expressions," *IEEE Access*, vol. 7, pp. 182701–182710, 2019.

[20] M. Mahdavi, H. H. Alhelou, N. D. Hatziargyriou, and A. Al-Hinai, "An efficient mathematical model for distribution system reconfiguration using AMPL," *IEEE Access*, vol. 9, pp. 79961–79993, 2021.

[21] Y. Qu, C. Liu, J. Xu, Y. Sun, S. Liao, and D. Ke, "A global optimum flow pattern for feeder reconfiguration to minimize power losses of unbalanced distribution systems," *Int. J. Electr. Power Energy Syst.*, vol. 131, Oct. 2021, Art. no. 107071.

[22] J. M. Home-Ortiz, R. Vargas, L. H. Macedo, and R. Romero, "Joint reconfiguration of feeders and allocation of capacitor banks in radial distribution systems considering voltage-dependent models," *Int. J. Electr. Power Energy Syst.*, vol. 107, pp. 298–310, Mar. 2019.

[23] U. Raut and S. Mishra, "An improved sine-cosine algorithm for simultaneous network reconfiguration and DG allocation in power distribution systems," *Appl. Soft Comput.*, vol. 92, Jul. 2020, Art. no. 106293.

[24] H. Teimourzadeh and B. Mohammadi-Ivatloo, "A three-dimensional group search optimization approach for simultaneous planning of distributed generation units and distribution network reconfiguration," *Appl. Soft Comput.*, vol. 88, Mar. 2020, Art. no. 106012.

[25] A. Jafar-Nowdeh, M. Babanezhad, S. Arabi-Nowdeh, A. Naderipour, H. Kamyab, Z. Abdul-Malek, and V. K. Ramachandaramurthy, "Meta-heuristic matrix moth-flame algorithm for optimal reconfiguration of distribution networks and placement of solar and wind renewable sources considering reliability," *Environ. Technol. Innov.*, vol. 20, Nov. 2020, Art. no. 101118.

[26] Y. Gupta, S. Doolla, K. Chatterjee, and B. C. Pal, "Optimal DG allocation and Volt–Var dispatch for a droop-based microgrid," *IEEE Trans. Smart Grid*, vol. 12, no. 1, pp. 169–181, Jan. 2021.

[27] M. Mohammadi, A. M. Rozbahani, and S. Bahmanyar, "Power loss reduction of distribution systems using BFO based optimal reconfiguration along with DG and shunt capacitor placement simultaneously in fuzzy framework," *J. Central South Univ.*, vol. 24, no. 1, pp. 90–103, Jan. 2017.

[28] H. B. Tolabi, A. L. Ara, and R. Hosseini, "A new thief and police algorithm and its application in simultaneous reconfiguration with optimal allocation of capacitor and distributed generation units," *Energy*, vol. 203, Jul. 2020, Art. no. 117911.

[29] V. B. Pamshetti, S. Singh, and S. P. Singh, "Combined impact of network reconfiguration and volt-VAR control devices on energy savings in the presence of distributed generation," *IEEE Syst. J.*, vol. 14, no. 1, pp. 995–1006, Mar. 2020.

[30] A. U. Rehman, Z. Wadud, R. M. Elavarasan, G. Hafeez, I. Khan, Z. Shafiq, and H. H. Alhelou, "An optimal power usage scheduling in smart grid integrated with renewable energy sources for energy management," *IEEE Access*, vol. 9, pp. 84619–84638, 2021.

[31] M. Premkumar, P. Jangir, R. Sowmya, R. M. Elavarasan, and B. S. Kumar, "Enhanced chaotic Jaya algorithm for parameter estimation of photovoltaic cell/modules," *ISA Trans.*, vol. 116, pp. 139–166, Jan. 2021.

[32] M. Ergezer, D. Simon, and D. Du, "Oppositional biogeography-based optimization," in *Proc. IEEE Int. Conf. Syst., Man Cybern.*, Oct. 2009, pp. 1009–1014.

[33] S. Li, H. Chen, M. Wang, A. A. Heidari, and S. Mirjalili, "Slime mould algorithm: A new method for stochastic optimization," *Future Gener. Comput. Syst.*, vol. 111, pp. 300–323, Oct. 2020.

[34] A. A. El-Fergany and A. Y. Abdelaziz, "Capacitor allocations in radial distribution networks using cuckoo search algorithm," *IET Gener., Transmiss. Distrib.*, vol. 8, no. 2, pp. 223–232, Feb. 2014.

[35] A. Zeinalzadeh, Y. Mohammadi, and M. H. Moradi, "Optimal multi objective placement and sizing of multiple DGs and shunt capacitor banks simultaneously considering load uncertainty via MOPSO approach," *Int. J. Electr. Power Energy Syst.*, vol. 67, pp. 336–349, May 2015.

[36] H. R. Tizhoosh, "Opposition-based learning: A new scheme for machine intelligence," in *Proc. Int. Conf. Comput. Intell. Modeling, Control Autom.*, 2005, pp. 695–701.
[37] S. Rahnamayan, H. R. Tizhoosh, and M. M. Salama, "Quasi-oppositional differential evolution," in *Proc. IEEE Congr. Evol. Comput.*, Sep. 2007, pp. 2229–2236.
[38] M. Ergezer and D. Simon, "Mathematical and experimental analyses of oppositional algorithms," *IEEE Trans. Cybern.*, vol. 44, no. 11, pp. 2178–2189, Nov. 2014.
[39] D. Zhang, Z.-C. Fu, and L.-C. Zhang, "An improved TS algorithm for loss-minimum reconfiguration in large-scale distribution systems," *Electr. Power Syst. Res.*, vol. 77, nos. 5–6, pp. 685–694, Apr. 2007.

SAUBHAGYA RANJAN BISWAL (Member, IEEE) received the B.Tech. degree in electrical and electronics engineering from the Silicon Institute of Technology, Bhubaneswar, India, in 2013, and the M.E. degree in power engineering from Jadavpur University, Kolkata, India, in 2016. He is currently pursuing the Ph.D. degree with the Department of Electrical Engineering, IIT (ISM) Dhanbad, India. His main research interests include power system optimization, distributed generation placement, optimal capacitor placement, and optimal reconfiguration of distribution systems.

GAURI SHANKAR (Member, IEEE) received the B.E. degree in electrical and electronics engineering from Birla Institute of Technology (BIT), Mesra, Ranchi, in 2003, the M.Tech. degree in energy studies from IIT Delhi, in 2005, and the Ph.D. degree in electrical engineering from IIT (ISM) Dhanbad, in 2016.

He started his teaching career as a Lecturer with the School of Engineering, University of Petroleum and Energy Studies, Dehradun, in 2005. He worked as an Assistant Professor with the Department of Electrical Engineering, North Eastern Regional Institute of Science and Technology (NERIST), a deemed university under MHRD, GoI, Itanagar, Arunachal Pradesh, from 2006 to 2010. He joined IIT (ISM) Dhanbad, in 2010, where he is currently working as an Assistant Professor with the Department of Electrical Engineering. He has several years of teaching experience. He is an active member of many journals, publishers, and conferences as a reviewer or an organizer. He has authored or coauthored over 50 publications, including journal articles, monographs, book chapters, and conference papers of repute. His research interests include power system operation and control, distributed generation, power quality issues in microgrid, and soft computing techniques.

RAJVIKRAM MADURAI ELAVARASAN received the B.E. degree in electrical and electronics engineering from Anna University, Chennai, India, and the M.E. degree (Hons.) in power system engineering from Thiagarajar College of Engineering, Madurai, India. He is a department topper and a gold medalist in his master's degree. He was an Technical Operations Associate with the IBM Global Technology Services Division. He was an Assistant Professor with the Department of Electrical and Electronics, Sri Venkateswara College of Engineering, Sriperumbudur, Chennai. He is currently holding various positions in academia and industry, which are as follows: a Visiting Scholar at the Clean and Resilient Energy Systems (CARES) Laboratory, Texas A&M University, Galveston, TX, USA, an Adjunct Faculty with the Department of Electrical and Electronics Engineering, Thiagarajar College of Engineering, and a Subject Matter Expert with the Power and Energy (Research and Development Unit), Nestlives Pvt. Ltd., Chennai. He has a Google citations of more than 1000. He has been a reviewer of more than 40 reputed SCIE journals. His research interests include renewable energy and smart grids, demand side management, multi criteria decision analysis, thermal energy storage, cyber-physical power systems, microgrids, power system operation and control, and artificial intelligence-based control techniques. He has more than 50 publications in SCIE journals.

LUCIAN MIHET-POPA (Senior Member, IEEE) was born, in 1969. He received the bachelor's degree in electrical engineering, the master's degree in electric drives and power electronics, and the Ph.D. and Habilitation degrees in electrical engineering from the Politehnica University of Timisoara, Romania, in 1999, 2000, 2002, and 2015, respectively. From 1999 to 2016, he was with the Politehnica University of Timisoara. He has also worked as a Research Scientist at the Technical University of Denmark, from 2011 to 2014, and Aalborg University, Denmark, from 2000 to 2002. He held a postdoctoral position at the University of Siegen, Germany, in 2004. Since 2016, he has been working as a Full Professor of energy technology with Østfold University College, Norway. He is currently the Head of the Research Laboratory "Intelligent Control of Energy Conversion and Storage Systems" and is one of the coordinators of the master's degree program in "Green Energy Technology" with the Faculty of Engineering, Østfold University College. He has published more than 130 articles in national and international journals and conference proceedings, and ten books. His research interests include modeling, simulation, control, and testing of energy conversion systems, and distributed energy resources (DER) components and systems, including battery storage systems (BSSs) [for electric vehicles and hybrid cars and vanadium redox batteries (VRB)] and energy efficiency in smart buildings and smart grids. He has served as a Scientific and Technical Program Committee Member for many IEEE conferences. He has participated in more than 15 international grants/projects, such as FP7, EEA, and Horizon 2020. He has been awarded more than ten national research grants. He was invited to join the Energy and Automotive Committees by the President and the Honorary President of the Atomium European Institute, working in close cooperation under the umbrella of EC and EU Parliament, and was also appointed as the Chairman of AI4People, Energy Section. Since 2017, he has been a Guest Editor of the Special Issues on *Energies* (MDPI), *Applied Sciences*, *Majlesi Journal of Electrical Engineering*, and *Advances in Meteorology* journals.